Integral Line-of-Sight Guidance of Underwater Vehicles Without Neutral Buoyancy ⋆

Martin S. Wiig [*,†] **Walter Caharija** [‡]
Thomas Røbekk Krogstad [†] **Kristin Y. Pettersen** [*,†]

[*] *Centre for Autonomous Marine Operations and Systems (NTNU AMOS), Department of Engineering Cybernetics, Norwegian University of Science and Technology (NTNU), Trondheim, Norway. E-mail: {Martin.Wiig, Kristin.Y.Pettersen}@itk.ntnu.no*
[†] *Norwegian Defence Research Establishment (FFI), Kjeller, Norway. E-mail: thomas-robekk.krogstad@ffi.no*
[‡] *Lloyd's Register Consulting - Energy AS, Trondheim, Norway. E-mail: walter.caharija@lr.org*

Abstract: This paper analyzes an integral line-of-sight guidance law applied to an underactuated underwater vehicle. The vehicle is rigorously modeled in 5 degrees of freedom using physical principles, and it is taken into account that the vehicle is not necessarily neutrally buoyant. The closed-loop dynamics of the cross-track error are analyzed using nonlinear cascaded systems theory, and are shown to achieve uniform semiglobal exponential stability. Hence, the integral line-of-sight guidance law compensates for the lack of neutral buoyancy, and it is no longer necessary to assume that the vehicle is perfectly ballasted. The exponential convergence properties of the guidance law are demonstrated in simulations of an autonomous underwater vehicle.

Keywords: path following, guidance systems, LOS guidance, underactuated vessel, disturbance compensation, exponentially stable, cascade control

1. INTRODUCTION

Guidance laws for underactuated marine vehicles makes it possible for vehicles equipped with fixed stern propellers and steering rudders to achieve control goals such as path following, tracking and maneuvering, described in Encarnação and Pascoal (2001), Breivik and Fossen (2009) and Fossen (2011). Precise path following is of particular importance in operations such as inspection of submarine pipelines, seabed mapping, and environmental monitoring.

The line-of-sight (LOS) path following principle, used in Healey and Lienard (1993), Pettersen and Lefeber (2001), Fossen et al. (2003), Breivik and Fossen (2004) and Fredriksen and Pettersen (2006), aims the vessel towards a point ahead on the path. Pettersen and Lefeber (2001) proved uniform global asymptotic and uniform local exponential stability (UGAS and ULES, or κ-exponential stability as defined in Sørdalen and Egeland (1995)) of the LOS guidance law in connection with a 3 degrees of freedom (3-DOF) vehicle model. A more complete vehicle model was included in Børhaug and Pettersen (2005) and Fredriksen and Pettersen (2006), while Fossen and Pettersen (2014) proved that the LOS guidance law achieves uniform semiglobal exponential stability (USGES), which gives stronger convergence and robustness properties.

⋆ This work was partly supported by the Research Council of Norway through the Centres of Excellence funding scheme, project no. 223254 - NTNU AMOS

Integral action was added to the LOS guidance law in Børhaug et al. (2008) to compensate for environmental kinematic disturbances such as ocean currents. The resulting integral line-of-sight (ILOS) guidance law for 3-DOF vehicles was proved to be globally κ-exponentially stable in Caharija et al. (2012a) and Caharija et al. (2014), and USGES and UGAS in Wiig et al. (2015).

ILOS guidance was applied to underwater vehicles modeled in 5-DOF in Caharija et al. (2012b) and Caharija et al. (2016), which added an ILOS guidance law in the vertical plane. The system was again shown to achieve κ-exponential stability.

All of the above mentioned works assume that the vehicle is neutrally buoyant, which requires perfect ballasting. In practice this can be difficult to achieve since water density changes with salinity, temperature and depth. This paper investigates the effect of positive or negative buoyancy on an underactuated underwater vehicle controlled by an ILOS guidance law. The 5-DOF kinematic and dynamic model used in Caharija et al. (2012b) and Caharija et al. (2016), which includes kinematic disturbances from constant and irrotational ocean currents, is extended to include effects caused by the lack of neutral buoyancy. The main contribution of the paper is to use the results of Fossen and Pettersen (2014) and Wiig et al. (2015) to prove that the closed-loop cross track error dynamics are

UGAS and USGES, even when the vehicle is not neutrally buoyant.

This paper is organized as follows: Section 2 gives a description of the vehicle model in 5-DOF, and states the control objective. Section 3 describes the ILOS guidance law and the surge, pitch and yaw controllers that are analyzed in this paper. The stability of the closed-loop system is analyzed in Section 4. Simulations demonstrating exponential stability are shown in Section 5, and some concluding remarks are given in Section 6.

2. SYSTEM DESCRIPTION

2.1 Basic assumptions

The following basic assumptions are used in the modeling and analysis of the system:

Assumption 1. The body-fixed coordinate frame b is located at a point $(x_g, 0, 0)$ from the vehicle's center of gravity (CG), along the center line of the vessel.

Assumption 2. The vehicle is passively stable in roll, and roll motion can hence be neglected.

Assumption 3. The difference between vehicle weight W and buoyancy B, defined as $W_E = W - B$, is assumed known and constant. Furthermore, CG and the center of buoyancy (CB) are located on the same vertical axis in b.

Remark 1. This is a relaxation of the neutral buoyancy assumption in previous works, such as Caharija et al. (2016).

Assumption 4. The vehicle is symmetric in the $x-z$ plane and has a large length to width ratio.

Assumption 5. The surge mode is decoupled from the other degrees of freedom, and only couplings in sway-yaw and heave-pitch are considered.

Assumption 6. The damping is considered linear.

Remark 2. The passive nature of nonlinear damping forces should enhance the directional stability of the vehicle, as noted in Caharija et al. (2016).

Assumption 7. The ocean current $\boldsymbol{v}_c \triangleq [V_x, V_y, V_z]^T$ in the inertial frame i is assumed to be constant, irrotational and bounded. Hence, there exists a constant $V_{\max} \geq 0$ such that $V_{\max} \geq \sqrt{V_x^2 + V_y^2 + V_z^2}$.

2.2 System Model

The vehicle is modeled in 5-DOF with $\boldsymbol{\eta} \triangleq [x, y, z, \theta, \psi]^T$ containing position and orientation in the inertial frame i. The velocity of the vessel in the body-fixed coordinate frame b is represented by $\boldsymbol{\nu} \triangleq [u, v, w, q, r]^T$, where u is surge speed, v is sway speed, w is heave speed, q is pitch rate and r is yaw rate.

The current velocity in the body frame b is $\boldsymbol{\nu}_c = \boldsymbol{R}^T(\theta,\psi)\boldsymbol{v}_c = [u_c, v_c, w_c]^T$, where $\boldsymbol{R}(\theta,\psi)$ is the rotation matrix from b to i given in (3). From Assumption 7 it follows that $\dot{\boldsymbol{v}}_c = \mathbf{0}$ and $\dot{\boldsymbol{\nu}}_c = [rv_c - qw_c, -ru_c, qu_c]^T$.

The vessel model is represented using velocities relative to the ocean current, as described in Fossen (2011). The body-fixed relative velocity is given by $\boldsymbol{\nu}_r \triangleq \boldsymbol{\nu} - \boldsymbol{\nu}_c = [u_r, v_r, w_r, q, r]^T$, where u_r, v_r and w_r are relative surge, sway and heave speed. The 5-DOF model of the vehicle is

$$\dot{\boldsymbol{\eta}} = \boldsymbol{J}(\boldsymbol{\eta})\boldsymbol{\nu}_r + \boldsymbol{\nu}_c, \tag{1a}$$
$$\boldsymbol{M}\dot{\boldsymbol{\nu}}_r + \boldsymbol{C}(\boldsymbol{\nu}_r)\boldsymbol{\nu}_r + \boldsymbol{D}\boldsymbol{\nu}_r + \boldsymbol{g}(\boldsymbol{\eta}) = \boldsymbol{B}\boldsymbol{f}, \tag{1b}$$

where $\boldsymbol{M} = \boldsymbol{M}^T > 0$ is the mass and inertia matrix including hydrodynamic added mass, the matrix $\boldsymbol{C}$ contains Coriolis and centripetal terms, and $\boldsymbol{D}(\boldsymbol{\nu}_r)$ is the hydrodynamic damping matrix. The matrix $\boldsymbol{B} \in \mathbb{R}^{5\times 3}$ is the actuator configuration matrix, while $\boldsymbol{f} \triangleq [T_u, T_q, T_r]^T$ is the control input vector with surge thrust T_u, pitch rudder angle T_q and yaw rudder angle T_r. The term $\boldsymbol{J}(\boldsymbol{\eta})$ is the velocity transformation matrix

$$\boldsymbol{J}(\boldsymbol{\eta}) \triangleq \begin{bmatrix} \boldsymbol{R}(\theta,\psi) & 0 \\ 0 & \boldsymbol{T}(\theta) \end{bmatrix}, \tag{2}$$

where $\boldsymbol{T}(\theta) \triangleq \mathrm{diag}(1, 1/\cos(\theta)), |\theta| \neq \frac{\pi}{2}$.

Following Assumption 3, the gravity restoration vector $\boldsymbol{g}(\boldsymbol{\eta}) \triangleq [W_E \sin(\theta), 0, -W_E\cos(\theta), (BG_z W + W_E z_b)\sin(\theta), 0]^T$, where BG_z is the vertical distance between CG and CB and z_b is the z-coordinate of the center of buoyancy in the body frame. Compared to the gravity restoration vector used in Caharija et al. (2016), the vector $\boldsymbol{g}(\boldsymbol{\eta})$ includes additional forces in surge and heave resulting from W_E, as well as an addition to the moment in pitch.

The matrix $\boldsymbol{C}$ is obtained from $\boldsymbol{M}$ as described in Fossen (2011), while the other system matrices can be expressed as:

$$\boldsymbol{R} \triangleq \begin{bmatrix} c_\psi c_\theta & -s_\psi & c_\psi s_\theta \\ s_\psi c_\theta & c_\psi & s_\psi s_\theta \\ -s_\theta & 0 & c_\theta \end{bmatrix}, \boldsymbol{D}_l \triangleq \begin{bmatrix} d_{11} & 0 & 0 & 0 & 0 \\ 0 & d_{22} & 0 & 0 & d_{25} \\ 0 & 0 & d_{33} & d_{34} & 0 \\ 0 & 0 & d_{43} & d_{44} & 0 \\ 0 & d_{25} & 0 & 0 & d_{55} \end{bmatrix},$$
$$\boldsymbol{M} \triangleq \begin{bmatrix} m_{11} & 0 & 0 & 0 & 0 \\ 0 & m_{22} & 0 & 0 & m_{25} \\ 0 & 0 & m_{33} & m_{34} & 0 \\ 0 & 0 & m_{43} & m_{44} & 0 \\ 0 & m_{25} & 0 & 0 & m_{55} \end{bmatrix}, \boldsymbol{B} \triangleq \begin{bmatrix} b_{11} & 0 & 0 \\ 0 & 0 & b_{23} \\ 0 & b_{32} & 0 \\ 0 & b_{42} & 0 \\ 0 & 0 & b_{53} \end{bmatrix}. \tag{3}$$

The terms $s. \triangleq \sin(\cdot)$ and $c. \triangleq \cos(\cdot)$ are used for brevity.

The structure of the system matrices is justified by Assumptions 2 - 6. The point x_g from Assumption 1 is chosen to lie on the pivot point of the ship, which gives $\boldsymbol{M}^{-1}\boldsymbol{B}\boldsymbol{f} = [\tau_u, 0, 0, \tau_q, \tau_r]^T$, where τ_u is the control force in surge, and τ_q and τ_r is the control moment in pitch and yaw.

2.3 System Model in Component Form

The 5-DOF model in (1) can be represented in component form:

$$\dot{x} = u_r c_\psi c_\theta - v_r s_\psi + w_r c_\psi s_\theta + V_x, \tag{4a}$$
$$\dot{y} = u_r s_\psi c_\theta + v_r c_\psi + w_r s_\psi s_\theta + V_y, \tag{4b}$$
$$\dot{z} = -u_r s_\theta + w_r c_\theta + V_z, \tag{4c}$$
$$\dot{\theta} = q, \tag{4d}$$
$$\dot{\psi} = r/c_\theta, \tag{4e}$$
$$\dot{u}_r = F_{u_r}(\theta, v_r, w_r, r, q) - \frac{d_{11}}{m_{11}}u_r + \tau_u, \tag{4f}$$
$$\dot{v}_r = X_{v_r}(u_r)r + Y_{v_r}(u_r)v_r, \tag{4g}$$

$$\dot{w}_r = X_{w_r}(u_r)q + Y_{w_r}(u_r)w_r + Z_{sw_r}s_\theta + Z_{cw_r}c_\theta, \quad (4h)$$

$$\dot{q} = F_q(\theta, u_r, w_r, q) + \tau_q. \quad (4i)$$

$$\dot{r} = F_r(u_r, v_r, r) + \tau_r. \quad (4j)$$

The terms F_{u_r}, X_{v_r}, Y_{v_r}, X_{w_r}, Y_{w_r}, Z_{sw_r}, Z_{cw_r}, F_q and F_r are defined in Appendix A. The lack of neutral buoyancy affects $\dot{u}_r$, $\dot{w}_r$ and $\dot{q}$ through F_{u_r}, Z_{sw_r}, Z_{cw_r} and F_q.

Assumption 8. For all $u_r \in [-V_{\max}, U_{rd}]$, where U_{rd} is the constant desired surge speed, the functions $Y_{v_r}(u_r)$ and $Y_{w_r}(u_r)$ satisfy

$$Y_{v_r}(u_r) \leq -Y_{\text{vr,min}} < 0, \quad (5)$$

$$Y_{w_r}(u_r) \leq -Y_{\text{wr,min}} < 0. \quad (6)$$

This ensures that the system is damped and nominally stable in sway and heave, which is the case for commercial vehicles.

2.4 Control objective

The objective of the control system is to make the vehicle modeled by (1) converge to and follow a straight-line path.

Assumption 9. The desired path $\mathcal{P}$ is horizontal.

Remark 3. A non-horizontal path will result in an additional bounded constant disturbance due to gravity, which the control system presented in this paper compensates for.

The path should be followed in the presence of unknown, constant and irrotational current while keeping a constant relative surge speed $U_{rd} > 0$. Without any loss of generality, the inertial reference frame i is placed such that its x-axis is aligned with the desired path, so that $\mathcal{P} \triangleq \{(x, y, z) \in \mathbb{R}^3 : y = 0, z = 0\}$. The objectives of the control system are formalized as

$$\lim_{t\to\infty} y(t) = 0, \ \lim_{t\to\infty} \psi(t) = \psi_{ss}, \ \psi_{ss} \in \left(-\frac{\pi}{2}, \frac{\pi}{2}\right), \quad (7a)$$

$$\lim_{t\to\infty} z(t) = 0, \ \lim_{t\to\infty} \theta(t) = \theta_{ss}, \ \theta_{ss} \in \left(-\frac{\pi}{2}, \frac{\pi}{2}\right), \quad (7b)$$

$$\lim_{t\to\infty} u_r(t) = U_{rd}, \quad (7c)$$

where ψ_{ss} and θ_{ss} is a constant yaw and heading angle required to keep the underactuated vessel at the path, compensating for a constant and irrotational ocean current, as well as for W_E.

The following assumption ensures that the vessel is able to follow the path for any direction of the ocean current:

Assumption 10. The desired relative surge speed U_{rd} is such that

$$U_{rd} > \max\left\{V_{\max} + \frac{5}{2}\frac{|Z_{sw_r}| + 0.5|Z_{cw_r}|}{|Y_{w_r}(U_{rd})|}, \ 2V_{\max} + 2\frac{|Z_{sw_r}| + 0.5|Z_{cw_r}|}{|Y_{w_r}(U_{rd})|}\right\}.$$

Note that Assumption 10 is stricter than the assumption on U_{rd} in Caharija et al. (2016). This is due to the presence of W_E in Z_{sw_r} and Z_{cw_r}.

3. CONTROL SYSTEM

This section presents a control system for the path following problem presented in Section 2.4.

3.1 The ILOS guidance law

The desired pitch θ_d and heading ψ_d are given by the ILOS guidance law introduced in Caharija et al. (2012b):

$$\theta_d \triangleq \tan^{-1}\left(\frac{z + \sigma_z z_{\text{int}}}{\Delta_z}\right), \quad \Delta_z > 0, \quad \sigma_z > 0, \quad (8a)$$

$$\dot{z}_{\text{int}} \triangleq \frac{\Delta_z z}{(z + \sigma_z z_{\text{int}})^2 + \Delta_z^2}, \quad (8b)$$

$$\psi_d \triangleq -\tan^{-1}\left(\frac{y + \sigma_y y_{\text{int}}}{\Delta_y}\right), \quad \Delta_y > 0, \quad \sigma_y > 0, \quad (8c)$$

$$\dot{y}_{\text{int}} \triangleq \frac{\Delta_y y}{(y + \sigma_y y_{\text{int}})^2 + \Delta_y^2}. \quad (8d)$$

The look-ahead distances Δ_z and Δ_y, and the integral gains σ_z and σ_y are constant design parameters. The auxiliary integral states z_{int} and y_{int} creates a nonzero desired heading and pitch even when the vehicle is on the path, making the vehicle counteract disturbances. The integral term growth rates (8b) and (8d) are designed to decrease for large cross-track errors z and y, reducing the risk of wind-up effects.

3.2 Surge, pitch and yaw controllers

Surge, pitch and yaw are controlled using feedback linearizing controllers along the lines of Caharija et al. (2016), and the surge controller has been extended with integral effect:

$$\tau_u = -F_{u_r}(v_r, w_r, \theta, r, q) + d_{11}U_{rd}/m_{11} - k_{u_r}(u_r - U_{rd}) - k_{i,u_r}\int_{t_0}^{t}(u_r - U_{rd}), \quad (9)$$

$$\tau_q = -F_q(\theta, u_r, w_r, q) + \ddot{\theta}_d - k_\theta(\theta - \theta_d) - k_q(q - \dot{\theta}_d), \quad (10)$$

$$\tau_r = -F_r(u_r, v_r, r) - q\sin(\theta)\dot{\psi} + \cos(\theta)\left[\ddot{\psi} - k_\psi(\psi - \psi_d) - k_r(\dot{\psi} - \dot{\psi}_d)\right]. \quad (11)$$

The control gains k_{u_r}, k_{i,u_r}, k_θ, k_q, k_ψ and k_r are constant and positive, and t_0 denotes the starting time. The integral term in the control law for τ_u has been added for robustness to modeling errors in the terms canceled out by F_{u_r}, e.g. the buoyancy error term W_E .

4. STABILITY OF THE CLOSED-LOOP SYSTEM

This section analyzes the stability properties of the complete vessel kinematics and dynamics. The terms $X_{w_r}^{U_{rd}} = X_{w_r}(U_{rd})$, $Y_{w_r}^{U_{rd}} = Y_{w_r}(U_{rd})$, $X_{v_r}^{U_{rd}} = X(U_{rd})$ and $Y_{v_r}^{U_{rd}} = Y(U_{rd})$ are used for brevity. Furthermore, the constants $\Gamma_{\max}$ and $\Gamma_{\inf}$ and the functions $\Gamma(\xi)$ and $\rho(\sigma_z)$ are defined as:

$$\Gamma(\xi) \triangleq U_{rd}\frac{1}{\sqrt{\xi^2 + 1}} - \frac{Z_{sw_r}\xi + Z_{cw_r}}{Y_{w_r}^{U_{rd}}}\frac{\xi}{\xi^2 + 1}, \quad (12)$$

$$\Gamma_{\inf} \triangleq \frac{1}{\sqrt{5}}U_{rd} - \frac{4}{5}\frac{|Z_{sw_r}| + 0.5|Z_{cw_r}|}{|Y_{w_r}^{U_{rd}}|}, \ \Gamma_{\max} \triangleq U_{rd}, \quad (13)$$

$$\rho(\sigma_z) \triangleq \frac{U_{rd} - V_{\max} - \sigma_z}{U_{rd} - V_{\max} - \sigma_z - \frac{5}{2}\frac{|Z_{sw_r}| + 0.5|Z_{cw_r}|}{|Y_{w_r}^{U_{rd}}|}}. \quad (14)$$

The constant ξ is defined in Section 4.1, where it is shown that $\Gamma_{\inf} < \Gamma(\xi) \leq \Gamma_{\max}$.

Theorem 1. If Assumptions 7 to 10 hold and the look-ahead distances Δ_y and Δ_z satisfy

$$\Delta_y > \frac{|X_{v_r}^{U_{rd}}|}{|Y_{v_r}^{U_{rd}}|}\left[\frac{5}{4}\frac{\Gamma_{\max}+V_{\max}+\sigma_y}{\Gamma_{\inf}-V_{\max}-\sigma_y}+1\right], \tag{15}$$

$$\Delta_z > \frac{|X_{w_r}^{U_{rd}}|}{|Y_{w_r}^{U_{rd}}|}\rho(\sigma_z)\left[\frac{5}{4}\frac{U_{rd}+V_{\max}+\sigma_z}{U_{rd}-V_{\max}-\sigma_z}+1\right], \tag{16}$$

and the integral gains σ_y and σ_z satisfy

$$0 < \sigma_y < \Gamma_{\inf} - V_{\max}, \tag{17}$$

$$0 < \sigma_z < U_{rd} - V_{\max} - \frac{5}{2}\frac{|Z_{sw_r}|+0.5|Z_{cw_r}|}{|Y_{w_r}^{U_{rd}}|}, \tag{18}$$

then the controllers (9) - (11) and guidance laws (8) guarantee achievement of the control objectives (7). The control objectives (7a)-(7b) are fulfilled with $\psi_{ss} = -\tan^{-1}(V_y/\sqrt{\Gamma(\xi)^2 - V_y^2})$ and $\theta_{ss} = \tan^{-1}(\xi)$. Furthermore, the equilibrium point of the error dynamics is USGES and UGAS.

Remark 4. The Z_{cw_r} term in the bound on U_{rd}, Δ_y, Δ_z, σ_y and σ_z is the result of the vehicle not being neutrally buoyant, as can be seen in the definition of Z_{cw_r} (A.6).

4.1 Proof of Theorem 1

The error signals of the actuated dynamics are collected in $\boldsymbol{\zeta} \triangleq [\tilde{u}_{\text{int}}, \tilde{u}_r, \tilde{\theta}, \tilde{q}, \tilde{\psi}, \tilde{r}]^T$, where $\tilde{u}_r \triangleq u_r - U_{rd}$, $\tilde{u}_{\text{int}} \triangleq \int_{t_0}^{t}(\tilde{u}_r)$, $\tilde{\theta} = \theta - \theta_d$, $\tilde{q} \triangleq q - \dot{\theta}_d$, $\tilde{\psi} = \psi - \psi_d$ and $\tilde{r} \triangleq r - \dot{\psi}_d$. The closed loop dynamics of $\boldsymbol{\zeta}$ are obtained by combining the system equations (4d), (4e), (4f), (4i) and (4j) with the control laws in surge (9), pitch (10) and yaw (11):

$$\dot{\boldsymbol{\zeta}} = \begin{bmatrix} 0 & 1 & 0 & 0 & 0 & 0 \\ -k_{i,u_r} & -(k_{u_r}+\frac{d_{11}}{m_{11}}) & 0 & 0 & 0 & 0 \\ 0 & 0 & 0 & 1 & 0 & 0 \\ 0 & 0 & -k_\theta & -k_q & 0 & 0 \\ 0 & 0 & 0 & 0 & 0 & 1 \\ 0 & 0 & 0 & 0 & -k_\psi & -k_r \end{bmatrix}\boldsymbol{\zeta} \triangleq \boldsymbol{\Sigma\zeta}. \tag{19}$$

The $z - w_r$ subsystem is obtained from (4c), (4h) and (8b):

$$\dot{z}_{\text{int}} = \frac{\Delta_z z}{(z+\sigma_z z_{\text{int}})^2 + \Delta_z^2}, \tag{20a}$$

$$\dot{z} = -u_r\sin(\tilde{\theta}+\theta_d) + w_r\cos(\tilde{\theta}+\theta_d) + V_z, \tag{20b}$$

$$\begin{aligned}\dot{w}_r = {} & X_{w_r}(\tilde{u}_r+U_{rd})(\tilde{q}+\dot{\theta}_d) + Y_{w_r}(\tilde{u}_r+U_{rd})w_r \\ & + Z_{sw_r}\sin(\tilde{\theta}+\theta_d) + Z_{cw_r}\cos(\tilde{\theta}+\theta_d).\end{aligned} \tag{20c}$$

Note that the buoyancy terms Z_{sw_r} and Z_{cw_r} show up in the underactuated heave dynamics (20c).

The calculation of the equilibrium point of (20) on the manifold $\boldsymbol{\zeta} = \mathbf{0}$ gives the equations

$$\xi\sqrt{\xi^2+1} = \frac{V_z}{U_{rd}}(\xi^2+1) - \frac{Z_{sw_r}\xi + Z_{cw_r}}{U_{rd}Y_{w_r}^{U_{rd}}}, \tag{21a}$$

$$w_r^{\text{eq}} = U_{rd}\xi - V_z\sqrt{\xi^2+1}, \tag{21b}$$

where $\xi \triangleq \sigma_z z_{\text{int}}^{\text{eq}}/\Delta_z$, and $z_{\text{int}}^{\text{eq}}$ and w_r^{eq} is the value of z_{int} and w_r at equilibrium.

Using the technique of (Caharija et al., 2016, Lemma IV.1) it can be shown that there exists at least one real solution for (21). Since the equilibrium point is later proven to be UGAS and USGES, the solution is unique. The steady state pitch angle is then $\theta_{\text{ss}} = \tan^{-1}(\xi)$. Furthermore, Assumption 10 can be used to give the following bound:

$$\left|\frac{V_z}{U_{rd}}(\xi^2+1) - \frac{Z_{sw_r}\xi + Z_{cw_r}}{U_{rd}Y_{w_r}^{U_{rd}}}\right| < \frac{1}{2}\left(\xi^2 + 3 + |\xi|\right) \tag{22}$$

Inserting (21a) into (22) and solving for $\xi_{\sup} > |\xi| > 0$ gives $\xi_{\sup} \approx 2$. Hence, $\Gamma_{\inf} < \Gamma(\xi) \leq \Gamma_{\max}$ holds, where $\Gamma(\xi)$ is defined in (12), and $\Gamma_{\inf}$ and $\Gamma_{\max}$ in (13).

A change of variables is introduced to obtain a system with the equilibrium point at the origin:

$$e_{z1} \triangleq z_{\text{int}} - z_{\text{int}}^{\text{eq}}, \quad e_{z2} \triangleq z + \sigma_z e_{z1}, \quad e_{z3} \triangleq w_r - w_r^{\text{eq}}. \tag{23}$$

After factorizing with respect to $\boldsymbol{\zeta}$, the interconnected dynamics of (19) and (20) can be expressed in cascade form as

$$\dot{\boldsymbol{e}}_z = \boldsymbol{A}_z(\boldsymbol{e}_z)\boldsymbol{e}_z + \boldsymbol{B}_z(\boldsymbol{e}_z) + \boldsymbol{H}_z(z, z_{\text{int}}, \theta_d, w_r, \boldsymbol{\zeta})\boldsymbol{\zeta}, \tag{24a}$$

$$\dot{\boldsymbol{\zeta}} = \boldsymbol{\Sigma\zeta}, \tag{24b}$$

where $\boldsymbol{e}_z \triangleq [e_{z1}, e_{z2}, e_{z3}]^T$, $\boldsymbol{A}_z$ is given in (26) while $\boldsymbol{B}_z$ is:.

$$\boldsymbol{B}_z \triangleq \begin{bmatrix} 0 \\ V_z f(e_{z2}) \\ \dfrac{\Delta_z X_{w_r}^{U_{rd}} V_z f(e_{z2})}{k_z(e_{z2})} - \dfrac{Z_{sw_r}\xi + Z_{cw_r}}{\sqrt{\xi^2+1}} f(e_{z2}) \end{bmatrix} \tag{25}$$

The interconnection matrix $\boldsymbol{H}_z$ contains all the terms vanishing at $\boldsymbol{\zeta} = 0$ and is given by

$$\boldsymbol{H}_z \triangleq \begin{bmatrix} 0 & 0 \\ 1 & 0 \\ \dfrac{\Delta_z\left(X_{w_r}(\tilde{u}+U_{rd}) - X_{w_r}^{U_{rd}}\right)}{k_z(e_{z2})} & 1 \end{bmatrix}\begin{bmatrix} \boldsymbol{h}_z^T \\ \boldsymbol{h}_{w_r}^T \end{bmatrix}, \tag{27}$$

where $\boldsymbol{h}_z$ and $\boldsymbol{h}_{w_r}$ are given in Appendix A. The term $k_z(e_{z2})$ is defined as

$$k_z(e_{z2}) \triangleq (e_{z2} + \sigma_z z_{\text{int}}^{\text{eq}})^2 + \Delta_z^2, \tag{28}$$

and $f(e_{z2})$ is defined as

$$f(e_{z2}) \triangleq 1 - \frac{\sqrt{(\sigma_z z_{\text{int}}^{\text{eq}})^2 + \Delta_z^2}}{\sqrt{k_z(e_{z2})}}. \tag{29}$$

Note that $f(e_{z2})$ is bounded by

$$|f(e_{z2})| \leq \frac{|e_{z2}|}{\sqrt{k_z(e_{z2})}}. \tag{30}$$

The nominal system of the cascade in (20) is

$$\dot{\boldsymbol{e}}_z = \boldsymbol{A}_z(\boldsymbol{e}_z)\boldsymbol{e}_z + \boldsymbol{B}_z(\boldsymbol{e}_z). \tag{31}$$

Lemma 2. Under the conditions of Theorem 1, the equilibrium point of the system (31) is UGAS and USGES.

Proof. The proof of Lemma 2 is given in Appendix B

Lemma 3. Under the conditions of Theorem 1, the equilibrium point of the complete system (24) is UGAS and USGES.

Proof. The system (24) is a cascaded system, consisting of a linear system (24b) which perturbs the dynamics (24a) through the interconnection matrix $\boldsymbol{H}_z$. The matrix $\boldsymbol{H}_z$ can be shown to satisfy $||\boldsymbol{H}_z|| \leq \delta_1(||\zeta||)(|z| + |z_{\text{int}}| + |w_r|) + \delta_2(||\zeta||)$, where $\delta_1(\cdot)$ and $\delta_2(\cdot)$ are some continuous non-negative functions.

The perturbing system (24b) is a linear, time-invariant system. Furthermore, since the gains k_{u_r}, k_{i,u_r}, k_ψ, k_r

$$\boldsymbol{A}_z \triangleq \begin{bmatrix} -\frac{\sigma_z \Delta_z}{k_z(e_{z2})} & \frac{\Delta_z}{k_z(e_{z2})} & 0 \\ -\frac{\sigma_z^2 \Delta_z}{k_z(e_{z2})} & -\frac{U_{rd}}{\sqrt{k_z(e_{z2})}} + \frac{\sigma_z \Delta_z}{k_z(e_{z2})} & \frac{\Delta_z}{\sqrt{k_z(e_{z2})}} \\ -\frac{\sigma_z^2 \Delta_z^2 X_{w_r}^{U_{rd}}}{k_z(e_{z2})^2} & \left(\frac{-U_{rd} \Delta_z X_{w_r}^{U_{rd}}}{k_z(e_{z2})^{3/2}} + \frac{\sigma_z \Delta_z^2 X_{w_r}^{U_{rd}}}{k_z(e_{z2})^2} + \frac{Z_{sw_r}}{\sqrt{k_z(e_{z2})}} \right) & \left(Y_{w_r}^{U_{rd}} + \frac{\Delta_z^2 X_{w_r}^{U_{rd}}}{k_z(e_{z2})^{3/2}} \right) \end{bmatrix} \tag{26}$$

and the term d_{11}/m_{11} are all strictly positive, the system matrix $\boldsymbol{\Sigma}$ is Hurwitz and the origin $\boldsymbol{\zeta} = \mathbf{0}$ is UGES.

The nominal system is USGES by Lemma 2. Hence all the conditions of (Loria and Panteley, 2004, Proposition 2.3) are satisfied, guaranteeing USGES and UGAS of the equilibrium point $(\boldsymbol{e}_z, \boldsymbol{\zeta}) = (\mathbf{0}, \mathbf{0})$ of (24). □

By Lemma 3, the control objective (7b) is achieved with exponential convergence properties and steady state pitch angle $\theta_{\text{ss}} = \tan^{-1}(\frac{\sigma_z z_{\text{int}}^{\text{eq}}}{\Delta_z})$. Let $\boldsymbol{\chi} = [\boldsymbol{e}_z^T, \boldsymbol{\zeta}^T]$ be a vector containing the exponentially converging error variables from (24). The complete vehicle kinematics and dynamics form a cascaded system where (24) perturbs the $y - v_r$ subsystem, which is obtained from (4b), (4g) and (8d):

$$\dot{y}_{\text{int}} = \frac{\Delta_y y}{(y + \sigma_y y_{\text{int}})^2 + \Delta_y^2}, \tag{32a}$$

$$\begin{aligned} \dot{y} = {} & u_r \sin(\tilde{\psi} + \psi_d) \cos(\tilde{\theta} + \theta_d) + v_r \cos(\tilde{\psi} + \psi_d) \\ & + w_r \sin(\tilde{\psi} + \psi_d) \sin(\tilde{\theta} + \theta_d) + V_y, \end{aligned} \tag{32b}$$

$$\begin{aligned} \dot{v}_r = {} & X_{v_r}(\tilde{u}_r + U_{rd}, \tilde{r} + r_d)(\dot{\tilde{\psi}} + \dot{\psi}_d) \cos(\tilde{\theta} + \theta_d) \\ & + Y_{v_r}(\tilde{u}_r + U_{rd}, v_r) v_r. \end{aligned} \tag{32c}$$

The equilibrium point of (32) on the manifold $\boldsymbol{\chi} = \mathbf{0}$ is given by

$$y_{\text{int}}^{\text{eq}} = \frac{\Delta}{\sigma} \frac{V_y}{\sqrt{\Gamma(\xi)^2 - V_y^2}}, \quad y^{\text{eq}} = 0, \quad v_r^{\text{eq}} = 0, \tag{33}$$

where $\Gamma(\xi)$ is defined in (12). A change of variables is introduced to obtain a system with the equilibrium point at the origin:

$$e_{y1} \triangleq y_{\text{int}} - y_{\text{int}}^{\text{eq}}, \; e_{y2} \triangleq y + \sigma e_{y1}, \; e_{y3} \triangleq v_r. \tag{34}$$

After factorizing with respect to $\boldsymbol{\chi}$ and substituting (8c) and (8a) for ψ_d and θ_d, the system in cascaded form becomes

$$\dot{\boldsymbol{e}}_y = \boldsymbol{A}_y \boldsymbol{e}_y + \boldsymbol{B}_y + \boldsymbol{H}_y(y, y_{\text{int}}, \theta_d, \psi_d, v_r, \boldsymbol{\chi}) \boldsymbol{\chi}, \tag{35a}$$

$$\dot{\boldsymbol{\chi}} = \begin{bmatrix} \boldsymbol{A}_z & \boldsymbol{H}_z \\ \mathbf{0} & \boldsymbol{\zeta} \end{bmatrix} \boldsymbol{\chi} + \begin{bmatrix} \boldsymbol{B}_z \\ \mathbf{0} \end{bmatrix} \tag{35b}$$

where $\boldsymbol{e}_y \triangleq [e_{y1}, e_{y2}, e_{y3}]^T$, $\boldsymbol{A}_y(e_{y2})$ is given in (37) while

$$\boldsymbol{B}_y(e_{y2}) \triangleq \begin{bmatrix} 0 \\ V_y f(e_{y2}) \\ -\frac{1}{\sqrt{\xi^2 + 1}} \frac{\Delta_y X_{v_r}^{U_{rd}} V_y}{k_y(e_{y2})} f(e2) \end{bmatrix}. \tag{36}$$

The interconnection matrix $\boldsymbol{H}_y$ contains all the terms vanishing at $\boldsymbol{\chi} = 0$ and is given by

$$\boldsymbol{H}_y \triangleq \begin{bmatrix} 0 & 0 \\ 1 & 0 \\ -\frac{\Delta_y \left(X_{v_r}(\tilde{u}_r + U_{rd}) - X_{v_r}^{U_{rd}} \right) \cos(\tilde{\theta} + \theta_d)}{k_y(e_{y2})} & 1 \end{bmatrix} \begin{bmatrix} \boldsymbol{h}_y^T \\ \boldsymbol{h}_{v_r}^T \end{bmatrix}, \tag{38}$$

where $\boldsymbol{h}_y$ and $\boldsymbol{h}_{v_r}$ are given in Appendix A. The term $k_y(e_{y2})$ is defined as

$$k_y(e_{y2}) \triangleq (e_{y2} + \sigma_y y_{\text{int}}^{\text{eq}})^2 + \Delta_y^2, \tag{39}$$

and $g(e_{y2})$ is defined as

$$g(e_{y2}) \triangleq 1 - \frac{\sqrt{(\sigma_y y_{\text{int}}^{\text{eq}})^2 + \Delta_y^2}}{\sqrt{k_y(e_{y2})}}, \tag{40}$$

which is bounded by

$$|g(e_{y2})| \leq \frac{|e_{y2}|}{\sqrt{k_y(e_{y2})}}. \tag{41}$$

Lemma 4. Under the conditions of Theorem 1, the origin of the system (35) is UGAS and USGES.

Proof. Consider the nominal system

$$\dot{\mathbf{e}}_y = \boldsymbol{A}_y(e_{y2}) + \boldsymbol{B}_y(e_{y2}). \tag{42}$$

This system is similar to the system (31), with the exception of the unknown constants ξ and $\Gamma(\xi)$. However, since $\Gamma(\xi)$ is bounded in (13), it is possible to apply Lemma 2 to conclude UGAS and USGES of the origin of (42). The origin of the perturbing system (35b) is shown in Lemma 3 to be UGAS and USGES as well. Finally, the interconnection matrix $\boldsymbol{H}_y$ can be shown to satisfy $||\boldsymbol{H}_y|| \leq \delta_3(||\boldsymbol{\chi}||)(|y| + |y_{\text{int}}| + |v_r|) + \delta_4(||\boldsymbol{\chi}||)$, where $\delta_3(\cdot)$ and $\delta_4(\cdot)$ are some continuous non-negative functions. Hence all the conditions of (Loria and Panteley, 2004, Proposition 2.3) are satisfied, guaranteeing USGES and UGAS of the equilibrium point $(\boldsymbol{e}_y, \boldsymbol{\chi}) = (\mathbf{0}, \mathbf{0})$ of (35). □

By Lemma 4, the control objective (7a) is achieved with exponential convergence properties and $\psi_{\text{ss}} = \tan^{-1}(V_y / \sqrt{\Gamma(\xi)^2 - V_y^2})$. Hence, all the control objectives are met and the proof of Theorem 1 is concluded.

5. SIMULATIONS

This section presents results from numerical simulations of the ILOS guidance law applied to an underactuated AUV modeled in 5-DOF. The AUV is tasked to follow a horizontal path along the x-axis. The desired relative surge speed is $U_{rd} = 2$ m/s. The current is $\boldsymbol{v}_c = [0.1 \text{ m/s}, 0.3 \text{ m/s}, 0.3 \text{ m/s}]$. The terms $Y_{v_r}^{U_{rd}}$ and $Y_{w_r}^{U_{rd}}$ are bounded by $Y_{\text{vr,min}} = Y_{\text{wr,min}} = 0.63 \text{ s}^{-1}$, and $|X_{v_r}^{U_{rd}}| = |X_{w_r}^{U_{rd}}| = 1.59 \text{ s}^{-1}$ and $|Y_{v_r}^{U_{rd}}| = |Y_{w_r}^{U_{rd}}| = 1.10 \text{ s}^{-1}$. The weight of the AUV is 1380 kg, which is 30 kg too heavy to be neutrally buoyant. This gives $Z_{sw_r} = 0.08 \text{ m}^2/\text{s}^2$ and $Z_{cw_r} = 0.14 \text{ m/s}^2$. The ILOS look-ahead distances and integral gains are $\Delta_y = \Delta_z = 10$ m and $\sigma_y = \sigma_z = 0.2$ m/s. The surge, yaw and pitch controllers (9)-(11) are implemented with $k_{u_r} = 0.5$, $k_{i,u_r} = 0.01$, $k_\psi = k_\theta = 1$ and $k_r = k_q = 2$. It can be confirmed that the conditions of Theorem 1, as well as all assumptions, are met.The initial position of the vehicle is 25 m east of and 25 m below the path, the initial direction is parallel to the path and the initial velocity is zero.

Figure 1 shows the track of the AUV in the $x - z$ plane. The vehicle maintains a constant sideslip and pitch angle

$$\boldsymbol{A}_y \triangleq \begin{bmatrix} -\frac{\sigma_y \Delta_y}{k_y(e_{y2})} & \frac{\Delta_y}{k_y(e_{y2})} & 0 \\ -\frac{\sigma_y^2 \Delta_y}{k_y(e_{y2})} & -\frac{\Gamma(\xi)}{\sqrt{k_y(e_{y2})}} + \frac{\sigma_y \Delta_y}{k_y(e_{y2})} & \frac{\Delta_y}{\sqrt{k_y(e_{y2})}} \\ \frac{1}{\sqrt{\xi^2+1}} \frac{\sigma_y^2 \Delta_y^2 X_{v_r}^{U_{rd}}}{k_y(e_{y2})^2} & \frac{1}{\sqrt{\xi^2+1}} \left(\frac{\Gamma(\xi) \Delta_y X_{v_r}^{U_{rd}}}{k_y(e_{y2})^{3/2}} - \frac{\sigma_y \Delta_y^2 X_{v_r}^{U_{rd}}}{k_y(e_{y2})^2} \right) & \left(Y_{v_r}^{U_{rd}} - \frac{\Delta_y^2 X_{v_r}^{U_{rd}}}{k_y(e_{y2})^{3/2} \sqrt{\xi^2+1}} \right) \end{bmatrix} \tag{37}$$

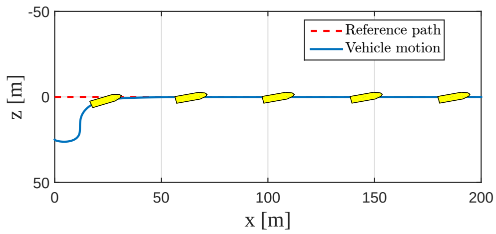

Fig. 1. Position and pitch of the vehicle in the $x - z$ plane during the simulation.

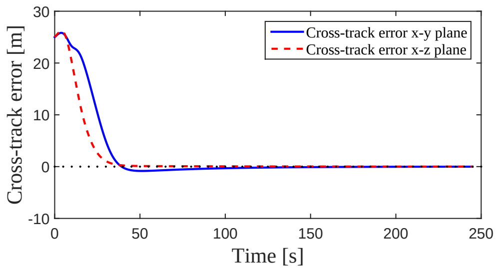

Fig. 2. The cross-track errors y and z of the vehicle.

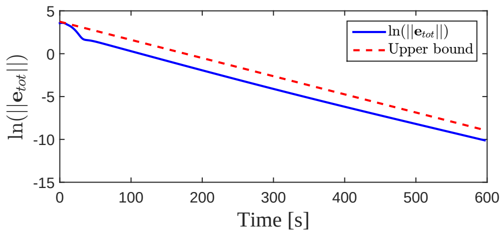

Fig. 3. The natural logarithm of $||\boldsymbol{e}_{\text{tot}}||$.

after converging to the path, counteracting the current and vehicle weight. The relative sway velocity v_r stabilizes at zero, while the relative heave velocity w_r stabilizes at 0.14 m/s due to the error in buoyancy and the moment induced by the distance between CG and CB. Figure 2 shows how the cross-track errors y and z converge to zero. Figure 3 shows the natural logarithm of the Euclidean norm of the error variables in (35), where $\boldsymbol{e}_{tot} \triangleq [\boldsymbol{e}_y^T, \boldsymbol{\chi}^T]^T$. Like in Wiig et al. (2015), the term $\ln(||\boldsymbol{e}_{\text{tot}}||)$ is upper bounded by a straight, descending line, corresponding to a bounding exponential function. Hence, for these initial conditions and parameters, exponential convergence of the system is verified.

In many scenarios, the difference between vehicle weight and buoyancy, W_E, will not be readily available. To investigate robustness with respect to W_E, the vehicle has been simulated with the negative buoyancy unknown to the controllers. Figure 4 shows the resulting $x - z$ track of the vehicle, which is still able to follow the path, though with slightly slower convergence.

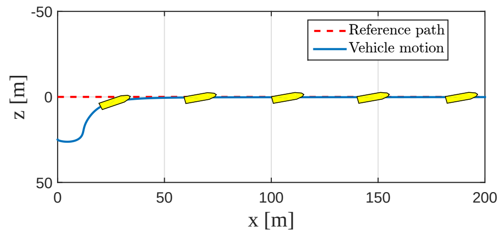

Fig. 4. Position and pitch of the vehicle in the $x - z$ plane when W_E is unknown to the controllers.

6. CONCLUSIONS

In this paper the stability properties of an underactuated underwater vehicle controlled by an ILOS guidance law have been investigated. Cascaded system analysis has been used to prove that the 5-DOF closed loop error dynamics are USGES, and this property is shown to hold also when the vehicle is not neutrally buoyant, which is often the case in practice. By achieving USGES, strong robustness properties of the system are guaranteed. A negatively buoyant AUV modeled in 5-DOF has been simulated in an ocean environment containing constant and irrotational current, demonstrating exponential stability of the closed loop error system. It is also demonstrated that the vehicle is able to follow the path, even when the negative buoyancy is unknown, which shows robustness of the system.

REFERENCES

Børhaug, E., Pavlov, A., and Pettersen, K.Y. (2008). Integral LOS control for path following of underactuated marine surface vessels in the presence of constant ocean currents. In *Proc. 47th IEEE Conference on Decision and Control*, 4984–4991. Cancun, Mexico.

Børhaug, E. and Pettersen, K.Y. (2005). Cross-track control for underactuated autonomous vehicles. In *Proc. 44th IEEE Conference on Decision and Control*, volume 2005, 602–608. Seville, Spain.

Breivik, M. and Fossen, T. (2004). Path following for marine surface vessels. In *Proc. Oceans '04 MTS/IEEE Techno-Ocean '04*, 2282–2289. Kobe, Japan.

Breivik, M. and Fossen, T.I. (2009). Guidance laws for autonomous underwater vehicles. In A.V. Inzartsev (ed.), *Intelligent Underwater Vehicles*, chapter 4, 51–76. I-Tech Education and Publishing, Vienna, Austria.

Caharija, W., Pettersen, K.Y., Sørensen, A.J., Candeloro, M., and Gravdahl, J.T. (2014). Relative velocity control and integral line of sight for path following of autonomous surface vessels: Merging intuition with theory. *Proc. Institution of Mechanical Engineers, Part M: Journal of Engineering for the Maritime Environment*, 228(2), 180–191.

Caharija, W., Candeloro, M., Pettersen, K.Y., and Sørensen, A.J. (2012a). Relative velocity control and integral LOS for path following of underactuated surface vessels. In *Proc. 9th IFAC Conference on Manuevering and Control of Marine Craft*, 380–385. Arenzano, Italy.

Caharija, W., Pettersen, K.Y., Bibuli, M., Calado, P., Zereik, E., Braga, J., Gravdahl, J.T., Sørensen, A.J., Milovanović, M., and Bruzzone, G. (2016). Integral line-of-sight guidance and control of underactuated marine vehicles: Theory, simulations and experiments. *IEEE Transactions on Control Systems Technology*, PP(99).

Caharija, W., Pettersen, K.Y., Gravdahl, J.T., and Børhaug, E. (2012b). Path following of underactuated autonomous underwater vehicles in the presence of ocean currents. In *Proc. 51st IEEE Conference on Decision and Control*, 528–535. Maui, HI, USA.

Encarnação, P. and Pascoal, A. (2001). Combined trajectory tracking and path following: An application to the coordinated control of autonomous marine craft. In *Proc. 40th IEEE Conference on Decision and Control*, December, 964–969. Orlando,FL.

Fossen, T.I. (2011). *Handbook of marine craft hydrodynamics and motion control*. John Wiley & Sons.

Fossen, T.I. and Pettersen, K.Y. (2014). On uniform semiglobal exponential stability (USGES) of proportional line-of-sight guidance laws. *Automatica*, 50(11), 2912–2917.

Fossen, T., Breivik, M., and Skjetne, R. (2003). Line-of-sight path following of underactuated marine craft. In *Proc. 6th IFAC Conference on Manoeuvring and Control of Marine Craft*, 244–249. Girona, Spain.

Fredriksen, E. and Pettersen, K. (2006). Global κ-exponential way-point maneuvering of ships: Theory and experiments. *Automatica*, 42(4), 677–687.

Healey, A. and Lienard, D. (1993). Multivariable sliding mode control for autonomous diving and steering of unmanned underwater vehicles. *IEEE Journal of Oceanic Engineering*, 18(3), 327–339.

Khalil, H.K. (2002). *Nonlinear Systems*. Pearson Education International inc., 3rd edition.

Loria, A. and Panteley, E. (2004). Cascaded nonlinear time-varying systems: analysis and design. In F. Lamnabhi-Lagarrigue, A. Loria, and E. Panteley (eds.), *Advanced Topics in Control Systems Theory*, chapter 2, 23–64. Springer Verlag, London.

Pettersen, K. and Lefeber, E. (2001). Way-point tracking control of ships. In *Proc. 40th IEEE Conference on Decision and Control*, 940–945. Orlando, FL.

Sørdalen, O.J. and Egeland, O. (1995). Exponential stabilization of nonholonomic chained systems. *IEEE Transactions on Automatic Control*, 40(1), 35–49.

Wiig, M.S., Pettersen, K.Y., and Krogstad, T.R. (2015). Uniform semiglobal exponential stability of integral line-of-sight guidance laws. In *Proc. 10th IFAC Conference on Manoeuvring and Control of Marine Craft*, 61–68. Copenhagen, Denmark.

Appendix A. FUNCTIONAL EXPRESSIONS

$$\begin{aligned} F_{u_r}(\theta, v_r, w_r, r, q) &\triangleq \frac{1}{m_{11}} \left[(m_{22}v_r + m_{25}r)r \right. \\ &\left. - (m_{33}w_r + m_{34}q)q - W_E \sin(\theta) \right] \end{aligned} \tag{A.1}$$

$$X_{v_r}(u_r) \triangleq \tfrac{m_{25}^2 - m_{11}m_{55}}{m_{22}m_{55} - m_{25}^2} u_r + \tfrac{d_{55}m_{25} - d_{25}m_{55}}{m_{22}m_{55} - m_{25}^2}, \tag{A.2}$$

$$Y_{v_r}(u_r) \triangleq \tfrac{(m_{22} - m_{11})m_{25}}{m_{22}m_{55} - m_{25}^2} u_r - \tfrac{d_{22}m_{55} - d_{52}m_{25}}{m_{22}m_{55} - m_{25}^2}, \tag{A.3}$$

$$X_{w_r}(u_r) \triangleq \tfrac{-m_{34}^2 - m_{11}m_{44}}{m_{33}m_{44} - m_{34}^2} u_r + \tfrac{d_{44}m_{34} - d_{34}m_{44}}{m_{33}m_{44} - m_{34}^2}, \tag{A.4}$$

$$Y_{w_r}(u_r) \triangleq \tfrac{(m_{11} - m_{33})m_{34}}{m_{33}m_{44} - m_{34}^2} u_r - \tfrac{d_{33}m_{44} - d_{43}m_{34}}{m_{33}m_{44} - m_{34}^2}, \tag{A.5}$$

$$Z_{sw_r} \triangleq \tfrac{(BG_zW + z_bW_E)m_{34}}{m_{33}m_{44} - m_{34}^2}, Z_{cw_r} \triangleq \tfrac{W_E m_{44}}{m_{33}m_{44} - m_{34}^2}, \tag{A.6}$$

$$\begin{aligned} &F_q(\theta, u_r, w_r, q) \triangleq -\tfrac{(BG_zW + z_bW_E)m_{33}}{m_{33}m_{44} - m_{34}^2} \sin(\theta) \\ &- \tfrac{W_E m_{34}}{m_{33}m_{44} - m_{34}^2} \cos(\theta) \\ &+ \tfrac{m_{34}d_{33} - m_{33}(d_{43} - (m_{33} - m_{11})u_r)}{m_{33}m_{44} - m_{34}^2} w_r \\ &+ \tfrac{m_{34}(d_{34} - m_{11}u_r) - m_{33}(d_{44} - m_{34}u_r)}{m_{33}m_{44} - m_{34}^2} q \end{aligned} \tag{A.7}$$

$$\begin{aligned} &F_r(u_r, v_r, r) \triangleq \tfrac{m_{25}d_{22} - m_{22}(d_{52} + (m_{22} - m_{11})u_r)}{m_{22}m_{55} - m_{25}^2} v_r \\ &+ \tfrac{m_{25}(d_{25} + m_{11}u_r) - m_{22}(d_{55} + m_{25}u_r)}{m_{22}m_{55} - m_{25}^2} r \end{aligned} \tag{A.8}$$

The vectors $\boldsymbol{h}_z \triangleq [\{h_{zi}\}]^T$ and $\boldsymbol{h}_{w_r} \triangleq [\{h_{w_r i}\}]^T, i = 1..6$, are defined as

$$h_{z2} = -\sin(\tilde{\theta} + \theta_d) \tag{A.9}$$

$$\begin{aligned} h_{z3} &= -U_{rd} \left[\tfrac{\sin(\tilde{\theta})}{\tilde{\theta}} \cos(\theta_d) + \tfrac{\cos(\tilde{\theta}) - 1}{\tilde{\theta}} \sin(\theta_d) \right] \\ &+ w_r \left[\tfrac{\cos(\tilde{\theta}) - 1}{\tilde{\theta}} \cos(\theta_d) - \tfrac{\sin(\tilde{\theta})}{\tilde{\theta}} \sin(\theta_d) \right], \end{aligned} \tag{A.10}$$

$$h_{z1} = h_{z4} = h_{z5} = h_{z6} = 0, \tag{A.11}$$

$$\begin{aligned} h_{w_r2} &= \tfrac{X_{w_r}(\tilde{u}_r + U_{rd}) - X_{w_r}^{U_{rd}}}{\tilde{u}_r} \gamma_{w_r}(z_{\text{int}}, z, w_r) \\ &+ \tfrac{Y_{w_r}(\tilde{u}_r + U_{rd}) - Y_{w_r}^{U_{rd}}}{\tilde{u}_r} w_r \end{aligned} \tag{A.12}$$

$$h_{w_r3} = Z_{sw_r} \left[\tfrac{\sin(\tilde{\theta})}{\tilde{\theta}} \cos(\theta_d) + \tfrac{\cos(\tilde{\theta}) - 1}{\tilde{\theta}} \sin(\theta_d) \right] \tag{A.13}$$

$$h_{w_r4} = X_{w_r}(\tilde{u}_r + U_{rd}), \tag{A.14}$$

$$h_{w_r1} = h_{w_r5} = h_{w_r6} = 0. \tag{A.15}$$

The vectors $\boldsymbol{h}_y \triangleq [\{h_{yi}\}]^T$ and $\boldsymbol{h}_{v_r} \triangleq [\{h_{v_r i}\}]^T, i = 1..9$, are defined as

$$\begin{aligned} h_{y2} &= \frac{U_{rd}}{e_{z2}} \left[\tfrac{\Delta_z}{\sqrt{k_z(e_{z2})}} - \tfrac{1}{\sqrt{\xi^2 + 1}} \right] \\ &- \tfrac{Z_{sw_r}\xi}{e_{z2} Y_{w_r}^{U_{rd}} \sqrt{\xi^2 + 1}} \left[\tfrac{e_{z2} + \sigma_z z_{\text{int}}^{\text{eq}}}{\sqrt{k_z(e_{z2})}} - \tfrac{\xi}{\sqrt{\xi^2 + 1}} \right], \end{aligned} \tag{A.16}$$

$$h_{y3} = \sin(\theta)\sin(\psi), h_{y5} = \cos(\theta)\sin(\psi) \tag{A.17}$$

$$\begin{aligned} h_{y6} &= U_{rd} \sin(\psi_d) \left[\tfrac{\cos(\tilde{\theta}) - 1}{\tilde{\theta}} \cos(\theta_d) - \tfrac{\sin(\tilde{\theta})}{\tilde{\theta}} \sin(\theta_d) \right] \\ &- \tfrac{Z_{sw_r}\xi \sin(\psi_d)}{Y_{w_r}^{U_{rd}} \sqrt{\xi^2 + 1}} \left[\tfrac{\sin(\tilde{\theta})}{\tilde{\theta}} \cos(\theta_d) + \tfrac{\cos(\tilde{\theta}) - 1}{\tilde{\theta}} \sin(\theta_d) \right] \end{aligned} \tag{A.18}$$

$$\begin{aligned} h_{y8} &= \left[U_{rd} \cos(\tilde{\theta} + \theta_d) - \tfrac{Z_{sw_r}\xi}{Y_{w_r}^{U_{rd}} \sqrt{\xi^2 + 1}} \sin(\tilde{\theta} + \theta_d) \right] \\ &\cdot \left[\tfrac{\sin(\tilde{\psi})}{\tilde{\psi}} \cos(\psi_d) + \tfrac{\cos(\tilde{\psi}) - 1}{\tilde{\psi}} \sin(\psi_d) \right] \\ &+ v_r \left[\tfrac{\cos(\tilde{\psi}) - 1}{\tilde{\psi}} \cos(\psi_d) - \tfrac{\sin(\tilde{\psi})}{\tilde{\psi}} \sin(\psi_d) \right] \end{aligned} \tag{A.19}$$

$$h_{y1} = h_{y4} = h_{y7} = h_{y9} = 0, \tag{A.20}$$

$$h_{v_r2} = \tfrac{X_{v_r}^{U_{rd}}}{e_{z2}} \left[\frac{\Delta_z}{\sqrt{k_z(e_{z2})}} - \frac{1}{\xi^2 + 1} \right] \gamma_{v_r}(y_{\text{int}}, y, y_r), \tag{A.21}$$

$$\begin{aligned} h_{v_r5} &= \tfrac{X_{v_r}(\tilde{u}_r + U_{rd}) - X_{v_r}^{U_{rd}}}{\tilde{u}_r} \cos(\tilde{\theta} + \theta_d) \gamma_{v_r}(y_{\text{int}}, y, y_r) \\ &+ v_r \tfrac{Y_{v_r}(\tilde{u}_r + U_{rd}) - Y_{v_r}^{U_{rd}}}{\tilde{u}_r} \end{aligned} \tag{A.22}$$

$$h_{v_r6} = \left[\tfrac{\cos(\tilde{\theta})-1}{\tilde{\theta}}\cos(\theta_d) - \tfrac{\sin(\tilde{\theta})}{\tilde{\theta}}\sin(\theta_d)\right] \cdot X_{v_r}^{U_{rd}}\gamma_{v_r}(y_{\text{int}}, y, y_r), \tag{A.23}$$

$$h_{v_r9} = X_{v_r}(\tilde{u}_r + U_{rd})\cos(\tilde{\theta} + \theta_d), \tag{A.24}$$

$$h_{v_r1} = h_{v_r3} = h_{v_r4} = h_{v_r7} = h_{v_r8} = 0. \tag{A.25}$$

The expressions $\gamma_{w_r}(z_{\text{int}}, z, w_r)$ and $\gamma_{v_r}(y_{\text{int}}, y, v_r)$ are defined as

$$\gamma_{w_r} \triangleq \tfrac{\Delta_z^2 w_r - \Delta_z U_{rd}(z+\sigma_z z_{\text{int}})}{k_z(e_{z2})^{3/2}} + \tfrac{\sigma_z \Delta_z^2}{k_z(e_{z2})^2} z + \tfrac{\Delta_z V_z}{k_z(e_{z2})}, \tag{A.26}$$

$$\gamma_{v_r} \triangleq \tfrac{\Delta_y \Gamma(\xi)(y+\sigma_y y_{\text{int}}) - \Delta_y^2}{k_y(e_{y2})^{3/2}} - \tfrac{\sigma_y \Delta_y^2}{k_y(e_{y2})^2} y - \tfrac{\Delta_y V_y}{k_y(e_{y2})}. \tag{A.27}$$

Appendix B. PROOF OF LEMMA 2

The proof follows along the lines of Caharija et al. (2016), while making use of the comparison lemma (Khalil, 2002, Lemma 3.4) along the lines of the analysis in Fossen and Pettersen (2014) and Wiig et al. (2015).

Consider the Lyapunov function candidate:

$$V \triangleq \tfrac{1}{2}\sigma^2 e_{z1}^2 + \tfrac{1}{2}e_{z2}^2 + \tfrac{1}{2}\mu e_{z3}^2, \quad \mu > 0. \tag{B.1}$$

Using (30) and Assumptions 7 and 8, the following bound can be found for $\dot{V}$:

$$\dot{V} \leq -W_1(\boldsymbol{e}_{z13}) - W_2(\boldsymbol{e}_{z23}), \tag{B.2}$$

where $\boldsymbol{e}_{z13} \triangleq [|e_{z1}|, |e_{z3}|]^T$ and $\boldsymbol{e}_{z23} \triangleq [|e_{z2}|, |e_{z3}|]^T$.

The function W_1 is defined as

$$W_1 = \frac{1}{k_z(e_{z2})}\boldsymbol{e}_{z13}^T \boldsymbol{Q}_1 \boldsymbol{e}_{z13}^T, \tag{B.3}$$

where $\boldsymbol{Q}_1$ is

$$\boldsymbol{Q}_1 \triangleq \begin{bmatrix} \sigma_z^3 \Delta_z & -\frac{\mu\sigma_z^2\sqrt{k_z(e_{z2})}|X_{w_r}^{U_{rd}}|}{2\Delta_z} \\ -\frac{\mu\sigma_z^2\sqrt{k_y(e_{y2})}|X_{w_r}^{U_{rd}}|}{2\Delta_z} & \mu\eta k_z(e_{z2})\left(|Y_{w_r}^{U_{rd}}| - \frac{|X_{w_r}^{U_{rd}}|}{\Delta_z}\right) \end{bmatrix} \tag{B.4}$$

and $0 < \eta < 1$. W_2 is defined as

$$W_2 \triangleq \frac{\Delta_z}{k_z(e_{z2})}\boldsymbol{e}_{z23}^T \boldsymbol{Q}_2 \boldsymbol{e}_{z23}, \tag{B.5}$$

where $\boldsymbol{Q}_2$ is

$$\boldsymbol{Q}_2 \triangleq \begin{bmatrix} \beta & -\alpha\sqrt{k_z(e_{z2})} \\ -\alpha\sqrt{k_z(e_{z2})} & k_z(e_{z2})\frac{\alpha(2\alpha-1)}{\beta} \end{bmatrix}. \tag{B.6}$$

Here, $\beta \triangleq U_{rd} - V_{\max} - \sigma_z$ and α is given by

$$\alpha \triangleq (1-\eta)\tfrac{(U_{rd} - V_{\max} - \sigma_z)(\Delta_z|Y_{w_r}^{U_{rd}}| - |X_{w_r}^{U_{rd}}|)}{|X_{w_r}^{U_{rd}}|(U_{rd} + V_{\max} + \sigma_z + \Delta_z \frac{2|Z_{sw_r}| + |Z_{cw_r}|}{|X_{w_r}^{U_{rd}}|})}. \tag{B.7}$$

The parameter μ is chosen as

$$\mu \triangleq \frac{2\alpha - 1}{\frac{|X_{w_r}^{U_{rd}}|}{\Delta_z^2}(U_{rd} + V_{\max} + \sigma_z) + \frac{2|Z_{sw_r}| + |Z_{cw_r}|}{\Delta_z}}. \tag{B.8}$$

If $\boldsymbol{Q}_1$ and $\boldsymbol{Q}_2$ are positive definite, then $\dot{V}$ is negative definite and the system (31) is uniformly stable. $\boldsymbol{Q}_1$ is positive definite if

$$\Delta_z > \frac{|X_{w_r}^{U_{rd}}|}{|Y_{w_r}^{U_{rd}}|}, \tag{B.9}$$

$$\mu < \frac{4\eta\Delta_z^2\left(\Delta_z|Y_{w_r}^{U_{rd}}| - |X_{w_r}^{U_{rd}}|\right)}{\sigma_z|X_{w_r}^{U_{rd}}|^2}. \tag{B.10}$$

(B.9) is met as long as (16) holds. It can be shown that $\eta \geq 1/5$ is a sufficient condition for μ to satisfy (B.10). Thus, without loss of generality, η is set to $1/5$, and positive definiteness of $\boldsymbol{Q}_1$ is ensured.

$\boldsymbol{Q}_2$ is positive definite if $\beta > 0$ and $\alpha > 1$. Assumption 10 and (18) ensure that $\beta > 0$, while conditions (16) and (18) ensure that $\alpha > 1$. Note that the presence of the buoyancy term Z_{cw_r} in $\boldsymbol{Q}_2$ influences the requirements on U_{rd} in Assumption 10, Δ_z in (16), and σ_z in (18).

With positive definite $\boldsymbol{Q}_1$ and $\boldsymbol{Q}_2$ it follows that $\dot{V} < 0$. Since $V > 0$, (Khalil, 2002, Theorem 4.8) shows that the equilibrium $\boldsymbol{e}_z = \boldsymbol{0}$ is uniformly stable.

The Lyapunov function candidate V from (B.1) is split into

$$V = V_1(\boldsymbol{e}_{z13}) + V_2(\boldsymbol{e}_{z23}), \tag{B.11}$$

where

$$V_1 \triangleq \tfrac{1}{2}\boldsymbol{e}_{z13}^T \boldsymbol{P}_1 \boldsymbol{e}_{z13}, \tag{B.12}$$

$$V_2 \triangleq \tfrac{1}{2}\boldsymbol{e}_{z23}^T \boldsymbol{P}_2 \boldsymbol{e}_{z23}, \tag{B.13}$$

the matrix $\boldsymbol{P}_1 = \text{diag}\left\{\sigma_z, \frac{1}{2}\mu\right\} > 0$ and $\boldsymbol{P}_2 = \text{diag}\left\{1, \frac{1}{2}\mu\right\} > 0$. Hence, using (B.3) and (B.5),

$$\dot{V}_1 \leq \frac{-2}{k_z(e_{z2})}\frac{q_{1,\min}}{p_{1,\max}}V_1, \tag{B.14}$$

$$\dot{V}_2 \leq \frac{-2\Delta_z}{k_z(e_{z2})}\frac{q_{2,\min}}{p_{2,\max}}V_2. \tag{B.15}$$

where $q_{i,\min} = \lambda_{\min}(\boldsymbol{Q}_i)$, $p_{i,\max} = \lambda_{\max}(\boldsymbol{P}_i)$, $i \in \{1, 2\}$. The function $1/k_z(e_{z2})$ can be bounded by bounding $\sigma_z z_{\text{int}}^{\text{eq}}$ using (21a):

$$\sigma_z z_{\text{int}}^{\text{eq}} = \frac{\xi}{\Delta_z} < \frac{\xi_{\text{sup}}}{\Delta_z} := \kappa, \tag{B.16}$$

where ξ_{sup} is the upper bound of ξ from Section 4.1. For each $r > 0$ and $|e_{z2}| \leq r$, the function $1/k_z(e_{z2})$ is then lower bounded by

$$\frac{1}{k_z(e_{z2})} \geq \frac{1}{(r+\kappa)^2 + \Delta_z^2} := c(r). \tag{B.17}$$

Inserting $c(r)$ into (B.14) and (B.15) gives

$$\dot{V}_1 \leq -2c(r)\tfrac{q_{1,\min}}{p_{1\max}}V_1, \ \forall ||\boldsymbol{e}_z(t)|| \leq r, \tag{B.18}$$

$$\dot{V}_2 \leq -2\Delta c(r)\tfrac{q_{2,\min}}{p_{2\max}}V_2, \ \forall ||\boldsymbol{e}_z(t)|| \leq r. \tag{B.19}$$

The inequalities in (B.18) and (B.19) are valid for all trajectories generated by the initial conditions $\boldsymbol{e}_z(t_0)$ since the system is uniformly stable. The comparison lemma can be invoked by noticing that the linear system $\dot{z} = -c(r)z$ has the solution $z(t) = e^{-c(r)(t-t_0)}z(t_0)$. This implies that for $v_1(t) = V_1(t, \boldsymbol{e}_z(t))$ and $v_2(t) = V_2(t, \boldsymbol{e}_z(t))$,

$$v_1(t) \leq e^{-2(q_{1,\min}/p_{1,\max})c(r)(t-t_0)}v_1(t_0), \tag{B.20}$$

$$v_2(t) \leq e^{-2(q_{2,\min}/p_{2,\max})\Delta_z c(r)(t-t_0)}v_2(t_0). \tag{B.21}$$

Consequently, for $v(t) = V(t, \boldsymbol{e}_z(t))$,

$$v(t) \leq e^{-2\vartheta c(r)(t-t_0)}v(t_0) \tag{B.22}$$

where $\vartheta = \min([q_{1,\min}/p_{1,\max}], [\Delta_z q_{2,\min}/p_{2,\max}])$. Therefore, with $p_{\max} \triangleq \max(\sigma^2, 1, \mu)$ and $p_{\min} \triangleq \min(\sigma^2, 1, \mu)$,

$$||\boldsymbol{e}_z(t)|| \leq \sqrt{\tfrac{p_{\max}}{p_{\min}}}e^{-\vartheta c(r)(t-t_0)}||\boldsymbol{e}_z(t_0)|| \tag{B.23}$$

Hence, the equilibrium point $\boldsymbol{e}_z = \boldsymbol{0}$ is USGES as defined in (Loria and Panteley, 2004, Definition 2.7).